Natural Resources Canada
Ressources naturelles Canada

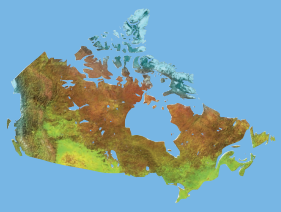

Capacitively coupled resistivity inversion using effective dipole lengths

G.A. Oldenborger and A.-M. LeBlanc

Geological Survey of Canada

Technical Note 6

2013

Canada

Geological Survey of Canada
Technical Note 6

Capacitively coupled resistivity inversion using effective dipole lengths

G.A. Oldenborger and A.-M. LeBlanc

2013

ISSN 1914-525X
Catalogue No. M41-10/6-2013E-PDF
ISBN 978-1-100-22557-9
doi:10.4095/292858

A copy of this publication is also available for reference in depository libraries across Canada through access to the Depository Services Program's Web site at http://dsp-psd.pwgsc.gc.ca

This publication is available for free download through GEOSCAN http://geoscan.ess.nrcan.gc.ca

Recommended citation

Oldenborger, G.A. and LeBlanc, A.-M., 2013. Capacitively coupled resistivity inversion using effective dipole lengths; Geological Survey of Canada, Technical Note 6, 7 p. doi:10.4095/292858

Critical review
J. Hunter

Authors
G.A. Oldenborger (Greg.Oldenborger@NRCan-RNCan.gc.ca)
A.-M. LeBlanc (Anne-Marie.LeBlanc@NRCan-RNCan.gc.ca)
Geological Survey of Canada
601 Booth Street
Ottawa, Ontario
K1A 0E8

Correction date:

Capacitively coupled resistivity inversion using effective dipole lengths

G.A. Oldenborger and A.-M. LeBlanc

Oldenborger, G.A. and LeBlanc, A.-M., 2013. Capacitively coupled resistivity inversion using effective dipole lengths; Geological Survey of Canada, Technical Note 6, 7 p. doi:10.4095/292858

Abstract: Noncontacting capacitively coupled resistivity (CCR) surveys find application in permafrost investigations and investigations over engineered surfaces. We have observed discrepancies between line-antenna CCR data and galvanic-resistivity (GR) data. Corresponding inverse models exhibit differences in both resistivity magnitude and structure. We have applied and tested the concept of effective dipole length for line-antenna CCR data collected over permafrost terrain in Iqaluit, Nunavut. We have compared inversions of corrected CCR data to the GR counterpart. Correcting CCR data with an effective dipole length of 80% of the physical antenna length results in a resistivity model most in accordance with the GR model. However, even after correction, the CCR model does not precisely emulate the GR model.

Résumé : Les levés de résistivité à couplage capacitif (RCC), effectués sans contact, sont utilisés dans les études de terrains pergélisolés et de surfaces artificielles. Nous avons observé des différences entre les données RCC obtenues avec des antennes à ligne d'alimentation et les données de résistivité galvanique (RG). Les modèles d'inversion de données correspondants présentent des différences dans l'amplitude et la structure de la résistivité. Nous avons appliqué et mis à l'essai le concept de la longueur effective du dipôle pour des données RCC recueillies avec des antennes à ligne d'alimentation sur un terrain pergélisolé à Iqaluit, au Nunavut. Nous avons comparé les inversions des données RCC corrigées à leurs équivalents RG. La correction des données RCC effectuée en utilisant une longueur effective du dipôle égale à 80 % de la longueur réelle de l'antenne produit le modèle de résistivité offrant la meilleure concordance avec le modèle RG. Par contre, même après cette correction, le modèle RCC n'imite pas précisément le modèle RG.

INTRODUCTION

The capacitively coupled resistivity (CCR) method is a geophysical method for measuring the electrical conductivity of the ground via noncontacting capacitive coupling of both the transmitting and receiving sensors. CCR history and theory is discussed in detail by Kuras et al. (2006). Much of modern CCR system development was carried out with the objective of mapping ground-ice occurrence in arctic regions as part of oil and gas prospecting and production (Timofeev et al., 1994; Hunter, 2007). The characteristics of CCR make it popular for applications in permafrost terrain or on engineered surfaces where either sensitivity to resistive materials is required, or achieving physical and electrical contact may be difficult or prohibitive (e.g. Fortier and Savard, 2010; Wilkinson et al., 2011).

Conceptually, acquisition and interpretation of CCR data is based upon understanding of the electrical-resistivity method with galvanic-electrode contact: DC resistivity or galvanic resistivity (GR). CCR sensor arrangement is based on a traditional GR array type, CCR data are transformed to apparent resistivity, and CCR data are typically inverted using electrode-based forward models and sensitivities. However, CCR instruments are typically operated at electromagnetic frequencies, and for CCR systems employing line antennas, the sensors are not point sources as is typically assumed for GR electrodes.

Hauck (2006) compared results for both survey types in permafrost terrain and observed that resistivities recovered via inversion were systematically different for the two systems; differences were attributed to frequency dependence of the electrical properties of ice. Oldenborger (2010) presented CCR and GR data collected along the same survey lines, with significant differences in both resistivity magnitude and interpretable features. However, those data were collected with different array types such that quantitative comparisons would be equivocal. During development of the VCHEP and RUSCAN systems, Timofeev was aware that apparent resistivity derived from line antennas did not match apparent resistivity data from grounded DC dipoles of the same length and that comparisons should be made to grounded DC dipoles of reduced length (Timofeev et al., 1994; J.A. Hunter, pers. comm., 2013). Kuras et al. (2006) showed that for homogeneous ground, line-antenna CCR data have an equivalent GR dipole length that is always shorter than the CCR antenna length and that this could result in incorrect representation of line-antenna data in electrode-based forward modelling and inversion algorithms. Neukirch and Klitzsch (2010) performed synthetic forward modelling and inversions to demonstrate that an effective dipole length could be used to achieve maximum similarity between sensitivities and inversion results for CCR and GR surveys.

Given the synthetic studies of Neukirch and Klitzsch (2010), we attempt to verify the effective dipole hypothesis and apply the results using field data from permafrost terrain in Iqaluit, Nunavut. CCR surveys in the region provide a pragmatic approach for characterization of permafrost terrain, where electrical resistivity can be high and information is required underneath roads, airport runways, and taxiways (LeBlanc et al., 2012).

METHODS

The OhmMapper is a commercially available CCR system developed by Geometrics Ltd. that has seen increased application in permafrost environments (Calvert, 2002; DePascale et al., 2008; Fortier and Savard, 2010). The OhmMapper system uses shielded coaxial cables as line antennas that couple a 16.5 kHz AC signal to the ground via the capacitance of the cable, where the antenna cable acts as one plate of the capacitor with the earth acting as the other (Groom, 2008). OhmMapper data are typically considered analogous to those from a GR survey with an in-line dipole-dipole geometry, but certain operating conditions must be satisfied.

Firstly, the effects of the imaginary conductivity or the real dielectric permittivity must be negligible such that any out-of-phase displacement currents are negligible and the transfer impedance is purely resistive. This is the quasi-static regime expressed as

$$\sigma >> 2\pi f \varepsilon \tag{1}$$

where σ is the real electrical conductivity, f is the frequency, and ε may include the effect of imaginary conductivity in addition to real dielectric permittivity.

In addition to the quasi-static regime, there must be no magnetic coupling; this condition is met by operating at a low induction number (e.g. McNeil, 1980). For the quasi-static regime, the induction number is a function of the skin depth given by

$$\delta = \sqrt{\frac{\rho}{\pi f \mu}} \tag{2}$$

where ρ is the electrical resistivity and μ is the permeability (of free space). Specific to the OhmMapper system, Groom (2008) suggests EM errors less than 2% for transmitter-receiver separations less than one skin depth. Corresponding operating conditions are

$$s < \sqrt{\frac{\rho}{\pi f \mu}} \quad \text{or} \quad \rho > \pi f \mu s^2 \tag{3}$$

where s is the centre-centre separation of the transmitting and receiving antennas and frequency is fixed. As such, the OhmMapper needs to be operated over sufficiently resistive ground, or with sufficiently small offsets. For extremely

resistive environments, operation may be outside of the quasi-static regime (e.g. Hauck, 2006), in which case the induction number is no longer applicable.

Even with the operating conditions satisfied, line-antenna CCR still differs from a GR experiment in terms of variation of current and voltage along the entire length of the line antennas. For line antennas, the transmitted current and received voltage are integral functions along the entire length. To account for this, the OhmMapper employs a line-antenna geometric factor

$$K_L = \frac{\pi a}{\ln\left[\left(\frac{b^2}{b^2-1}\right)^{2b}\left(\frac{b^2+2b}{(b+1)^2}\right)^{b+2}\left(\frac{b^2-2b}{(b-1)^2}\right)^{b-2}\right]} \qquad (4)$$

where $b = 2s/a$ and a is the antenna length (Kuras et al., 2006; Groom, 2008). The OhmMapper resistance data are transformed to dipole-dipole apparent-resistivity data with dipole length a, dipole distance $d = s–a$, and n-spacing $n = d/a$. However, Kuras et al. (2006) showed that even with the line-antenna geometric factor, CCR measurements have an equivalent GR counterpart with an effective dipole length that is as short as $0.5a$ over a homogeneous halfspace. Neukirch and Klitzsch (2010) analyzed the synthetic sensitivities, apparent resistivities, and inversion results for a line-antenna CCR system with effective dipole lengths of $0.5a$ and $0.8a$ and concluded that OhmMapper data should be corrected for dipole lengths of $0.8a$. We apply the effective dipole length concept to field data and compare to a GR survey.

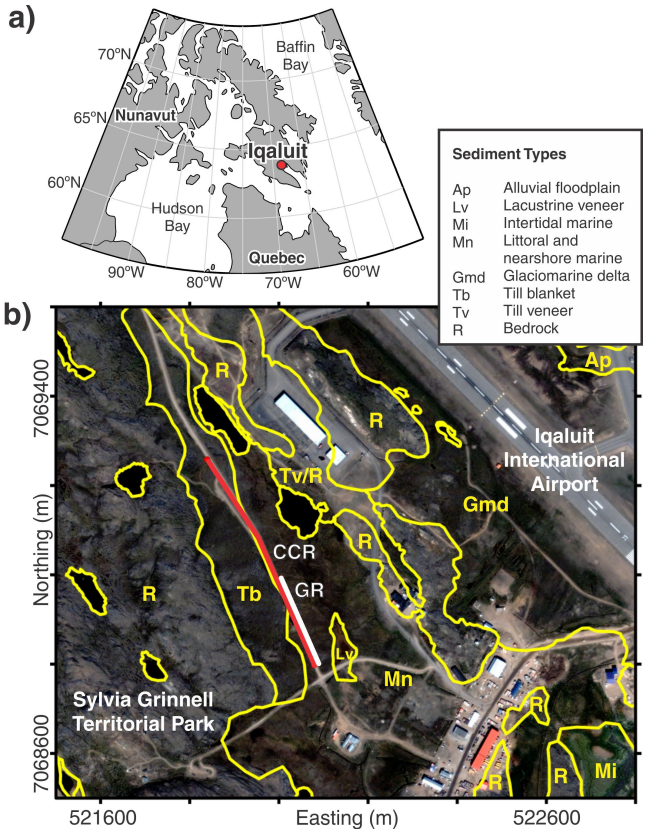

Figure 1. a) Location map for Iqaluit, Nunavut, at the head of Frobisher Bay. **b)** Locations of CCR (red) and GR (white) survey lines. Inset legend gives a description of the sediment types for the mapped surficial geology of the area (Allard et al., 2012). QuickBird satellite image, July 25 2006, © DigitalGlobe Inc., all rights reserved.

Data collection

We utilize CCR and GR data collected in August 2010 as part of permafrost-terrain characterization activities in Iqaluit, Nunavut (Allard et al., 2012; LeBlanc et al., 2013). The CCR data were collected along 500 m of an unsurfaced road in Sylvia Grinnell Territorial Park (Fig. 1) using an OhmMapper system with 5 receiving antennas of 5 m length and dipole distances (rope lengths) of 2.5, 15, 25, and 30 m (n-spacings of 0.5–8). GR data were collected along a 200 m section of the CCR data set using an IRIS SYSCAL R1 Plus system.

Designing an exactly equivalent GR survey is difficult. Firstly, there is the issue of signal integration along the line antenna and the associated uncertainty as to what the equivalent four-electrode dipole lengths should be. Furthermore, OhmMapper data are collected at a constant sample rate, not at specified spatial intervals. Data are subsequently averaged to a nominal electrode spacing and the resulting data density can be high.

In light of these differences, the GR survey was conducted with 3 m electrode spacing and the OhmMapper data were averaged to a nominal electrode spacing of 2.5 m. The GR spacing was chosen to best emulate the effect of integration along the 5 m line antennas and it represents a compromise between the effective dipole lengths of $0.5a$ and $0.8a$ (or 2.5 m and 4 m). We intend to ultimately compare inversion results in model space such that exact replication of the data is not required (and not likely possible).

The GR data were collected as a standard 3 m dipole-dipole survey with n-spacings of 1 to 6. Additional GR data were collected using 9 m dipoles with n-spacings of 2, 8/3, 10/3, 4, 14/3, 16/3, and 15 m dipoles with n-spacings of 16/5, 18/5, 4, 22/5, 24/5, 26/5. The larger dipole GR data allow comparison to the higher n-spacing CCR data. From a pragmatic point of view, we want to determine which effective CCR dipole length results in the best recovery of the 'true' earth model, not which CCR dipole length best matches the model recovered from an admittedly limited GR data set. To this end, the model recovered from both small and large dipole GR data will be used as the judgment model.

To compare results, we first consider the CCR apparent resistivity ρ_a given the physical antenna length a, dipole distances d, and n-spacings. We then define an effective dipole length as $a' = pa$ where $p = 0.5$ or $p = 0.8$ is the relative length

factor, as per Neukirch and Klitzsch (2010). This results in an effective dipole distance and n-spacing of $d' = d+a-a'$ and $n' = d'/a'$, although the dipole-dipole separation and midpoints remain unchanged. The effective geometric factor K_L' is calculated using $b' = 2s/a'$. We can recover the measured transfer resistance as $R_L = \rho_a/K_L$ and correct the apparent resistivity, or we can directly correct the apparent resistivity as

$$\rho_a' = \frac{K_L'}{K_L}\rho_a \tag{5}$$

The corrected data sets are compared to the GR data and then inverted. Results are compared to the GR model.

RESULTS

A direct comparison of the GR and CCR data is not possible due to the purposefully different survey geometries. Direct comparison of the original and corrected CCR data is also problematic because modification of the dipole length changes the effective array geometry. Nevertheless, we select data with approximately equivalent median depths of exploration as defined by Edwards (1977). Figure 2 shows the GR data at n = 4, the CCR data at n = 2, the CCR data for p = 0.8 at n' = 2.75, and the CCR data for p = 0.5 at n' = 5.0; these data subsets correspond to depths of 3.5, 3.6, 3.5, and 3.7 m, respectively. The scaling ratios K_L'/K_L for the corrected CCR data are approximately 1.6 and 4.2. CCR apparent resistivities are lower than GR apparent resistivities for equivalent exploration depths. Qualitatively, the p = 0.5 correction appears to provide a good match to the GR data, with the p = 0.8 correction perhaps doing a better job over some resistive ground. Regardless, at almost all locations, either correction results in a better match to the GR data than the original CCR data.

Both the GR and CCR data were inverted using the iteratively reweighted least-squares method of Loke et al. (2003). Data with greater than 10% misfit were reweighted to reduce the effect of outliers, and a large Ekblom perturbation of 0.5 was used to approximate a 'soft' L_1 norm on the model (Farquharson and Oldenburg, 1998). The recovered models are relatively robust to small changes in inversion settings, and the conclusions based on relative comparisons should hold for small departures from the 'best' models. The model grids are nearly equivalent for the various data sets, with surface cell sizes of 1.5 m horizontal by 0.75 m vertical for the GR data and the p = 0.8 CCR data, and 1.25 m horizontal by 0.625 m vertical for the p = 1.0 and p = 0.5 CCR data. Minimal smoothing has been applied to the CCR data in order to not obfuscate effects of correction, and the same inversion settings have been applied to the GR and CCR data sets, although different noise levels result in different convergence behaviour and different levels of convergence (damping) mean necessarily different resolution regardless of effective dipole length.

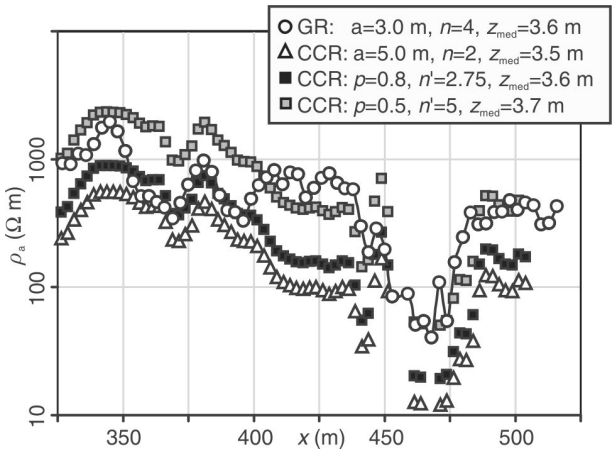

Figure 2. Apparent resistivity as a function of array midpoint for GR data, CCR data, and corrected CCR data at approximately equal median depths of exploration. ρ_a = apparent resistivity, x = array midpoint, a = dipole length, n = n-spacing, z_{med} = median depth of exploration, p = relative length factor, n' = effective n-spacing.

Figure 3 shows a comparison of GR and CCR inversion results. There is no indication in the convergence behaviour of the inversions as to which CCR correction factor is most appropriate; we do not observe any faster convergence or lower misfit that might be attributed to better adherence to the electrode-based physics of the forward model. The CCR misfit is much higher than the GR misfit, as expected given the higher noise levels observed for CCR data (Hauck, 2006; Oldenborger, 2010). Inversion misfit and model noise could be reduced by trimming high-misfit data and re-inverting, but this might obscure the effectiveness of CCR correction.

In general, the model structures are similar for each data set, but the CCR model under-predicts the resistivity (Fig. 3b). This is in agreement with the observations of Hauck (2006). Furthermore, the CCR model exhibits a resistive surface layer that is thinner than the GR surface layer, although the CCR model does capture the thinning of the resistive surface layer from north to south and the conductive 'window' at approximately 465 m line position. The deep resistive GR anomaly at approximately 415 m line position appears shallower and more laterally extensive in the CCR model, and the deep resistive GR anomaly at approximately 460 m is missing from the CCR model.

Correction of the CCR data for effective dipole length results in resistivity values more in agreement with the GR model, with a general increase from the p = 0.8 correction (Fig. 3c) to the p = 0.5 correction (Fig. 3d). However, Figure 3 also shows that the changes in model space resulting from correction are not necessarily monotonic and may be strongly nonlinear in places. In particular, the p = 0.8 correction results in the recovery of a deep resistive anomaly at approximately 475 m line position that may correspond to the GR model. Furthermore, the p = 0.8 correction results in more thinning of the middle conductive layer than the p = 0.5 correction.

DISCUSSION

As evidenced by the comparison of GR and CCR models recovered from field data, establishing the most appropriate correction factor is difficult. The models are sufficiently complex that a 1:1 comparison of recovered resistivity model parameters is not informative. Figure 4 shows the histogram distributions of model resistivity for regridding of the recovered resistivity models onto a common grid. The histograms clearly show that the model recovered from the original CCR data is skewed to low resistivities. The model recovered from the $p = 0.5$ CCR data is skewed to high resistivities, as is the model recovered from the $p = 0.8$ CCR data, although not to the same extent. The bimodal nature of the GR distribution is less apparent in the CCR distributions, but is best represented by the $p = 0.8$ distribution.

Inversion results of field data show that for any single correction factor, recovered model resistivities may be both under- and over-corrected with respect to the GR model. Nevertheless, the $p = 0.8$ effective dipole length appears to provide the best compromise. Further, the $p = 0.8$ CCR model (Fig. 3c) is the only CCR model that exhibits a double resistive anomaly at depth consistent with the GR model (Fig. 3a).

The uniform convergence behaviour and high final data misfits encountered during inversions of all the CCR data sets suggest that discrepancies between inversions of GR and CCR data are not solely associated with the line-antenna nature of the data in an electrode-based inversion algorithm; other candidates for causing high misfits are generally higher levels of background noise and position errors (Oldenborger et al., 2005) that could result from time-based data acquisition and position averaging.

Furthermore, recovered resistivities are relatively low given the permafrost environment. We are well within the quasi-static regime, but there is reason to be concerned about violation of the low–induction-number condition. At 5 Ω m, $s<\delta$ is satisfied only at $n = 0.5$ or $d = 2.5$ for 5 m dipoles. At 100 Ω m, $s<\delta$ is satisfied out to $n = 6$ or $d = 30$ m and at 200 Ω m, $s<\delta$ is satisfied past $n = 8$ or $d = 40$ m, which is the maximum

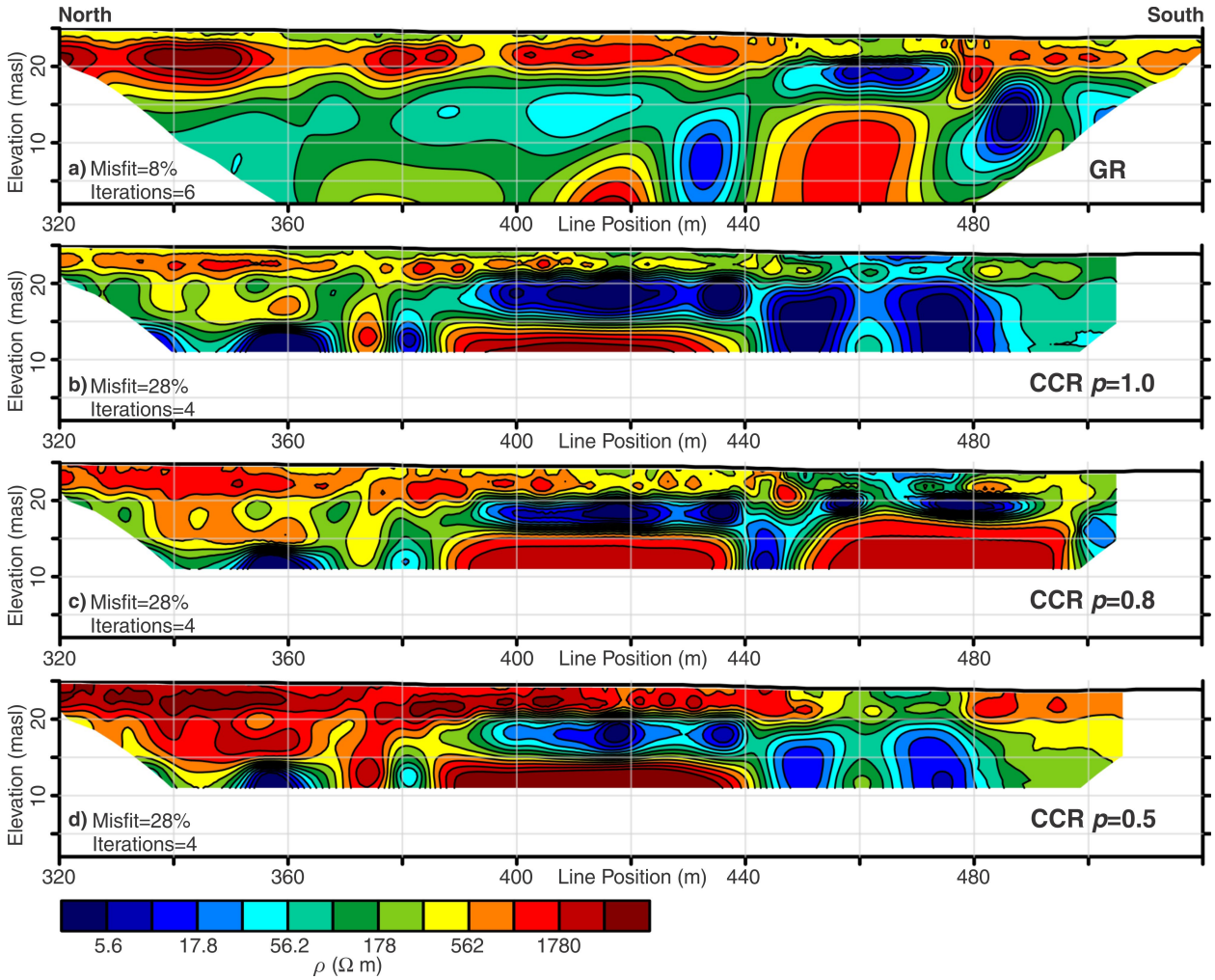

Figure 3. Electrical-resistivity models recovered from inversion of **a)** GR data, **b)** CCR data, **c)** $p = 0.8$ corrected CCR data, and **d)** $p = 0.5$ corrected CCR data. masl = metres above sea level, p = relative length factor, ρ = electrical resistivity. Vertical exaggeration = 1.5x.

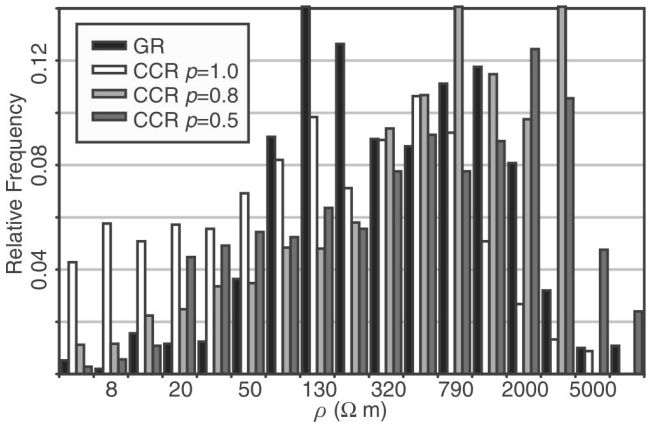

Figure 4. Histogram of recovered electrical resistivity for GR data, CCR data, and corrected CCR data for the common model limits of 340–500 m line position and 12–23 m elevation. ρ = electrical resistivity, p = relative length factor.

dipole distance for the experiment in question. Given the heterogeneity of the ground, the effective conductivity is not unique. For most measurements, the low–induction-number condition is likely satisfied, but electromagnetic effects cannot be ruled out as a source of noise, particularly for large dipole separations that are further affected by increased conductivity at depth (especially at the southern end of the section). During acquisition, CCR signal loss was noted for large dipole separations at the southern end of the section, which is consistent with an increase in ground conductivity and a reduction of skin depth. At s = 30 m, $s<\delta$ is violated for resistivities of approximately 60 Ω m or less, which is consistent with resistivities recovered at depth in the GR model (Fig. 3a).

Model interpretation

Figure 5 shows the resistivity model recovered from the correction of the entire CCR data set using a p = 0.8 effective dipole length. We interpret the thin active layer (1–1.5 m thick) to be manifested as the slight transition to lower resistivities at the surface of the model. Distinct imaging of the active layer is not possible with these data. Bedrock topography in the region is observed to be quite variable, and we consider the resistive anomalies at the southern end of the section to be indicative of bedrock highs. Resolution at depth is limited and we do not expect to be able to distinguish a strong versus moderate resistor. The marine sediments (Mn, Fig. 1) are largely silty to gravelly sand, consistent with the observed resistivity (Scott et al., 1990). The till blanket (Tb, Fig. 1) has a silty-sand matrix and appears only slightly more conductive than the marine sediments. However, at depth, we image a conductive material that is not identified on surficial maps. This is interpreted to be the manifestation of fine-grained marine sediments with potentially saline porewater. Such sediments are significant when considering subsidence potential associated with permafrost degradation and infrastructure. We hope to correlate this conductive unit with similar conductive anomalies observed around the Iqaluit area (LeBlanc et al., 2012). Before correction of the CCR data, correlation of this anomaly was uncertain due to its apparently lower resistivity, equivalent to that of the resistivity recovered for GR data collected over the modern saturated tidal flats of Frobisher Bay.

CONCLUSIONS

For the inversion of line-antenna CCR data, an effective dipole-length correction factor of p = 0.8 results in recovered model resistivities and model structure that are most consistent with a GR model obtained over the same region. There is likely no single optimal correction factor, and a p = 0.5 correction also generates a resistivity model that is more consistent with the GR model than without a correction. We consider a p = 0.8 correction to be prudent, especially for investigations involving multiple data types where correlation or comparison of resistivities is required, or for situations where estimation or discrimination of subtle material types is desirable.

Resistivity models recovered from CCR data will likely never precisely emulate those recovered from GR data, due to the inherent differences in field-measurement procedures and noise levels. Even with effective dipole-length correction, significant discrepancies exist between CCR and GR

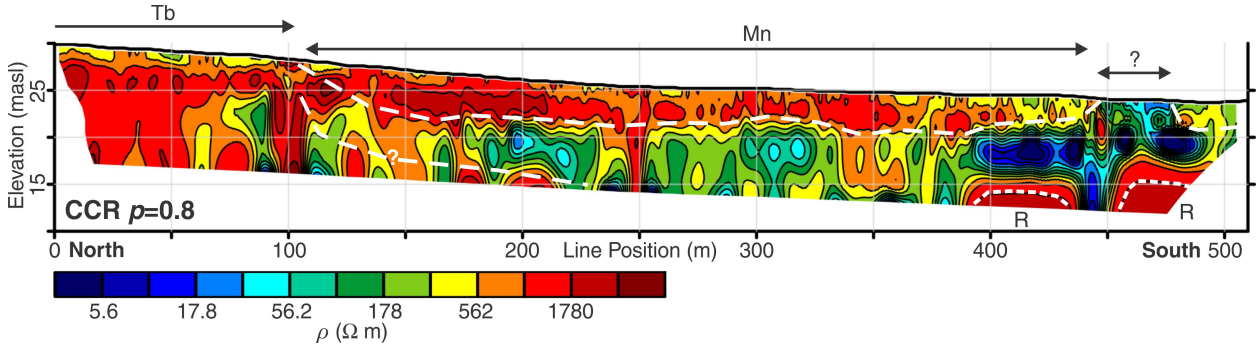

Figure 5. Interpreted electrical-resistivity model for p = 0.8 corrected CCR data. Identified units correspond to Figure 1 legend. The question mark indicates an unmapped unit hypothesized to be fine-grained marine sediments. The lower boundary of this unit is uncertain at the northern end of the section. ρ = electrical resistivity, p = relative length factor, masl = metres above sea level. Vertical exaggeration = 4x.

models for the same region. We consider a model-space calibration to be most pragmatic, and we should strive to compare experiments with equivalent resolution. However, quantifying the true resolution of a line-antenna survey is not straightforward, and anticipation of disparate noise levels is problematic. Furthermore, given the nonlinearity of the problem, results may be a function of the model (or field site) under consideration.

ACKNOWLEDGMENTS

This work was conducted as part of the Climate Change Geoscience Program, Natural Resources Canada. Additional funding was provided by the Canada-Nunavut Geoscience Office (CNGO). Fieldwork was conducted with assistance from P. Gosselin, A.-S. Carbonneau, J. Doyon, and the CNGO. A constructive review was provided by J.A. Hunter.

REFERENCES

Allard, M., Doyon, J., Mathon-Dufour, V., LeBlanc, A.-M., L'Hérault, E., Mate, D., Oldenborger, G.A., and Sladen, W.E., 2012. Surficial geology, Iqaluit, Nunavut; Geological Survey of Canada, Canadian Geoscience Map 64 (preliminary), scale 1:15 000. doi:10.4095/289503

Calvert, H.T., 2002. Capacitive-coupled resistivity survey of ice-bearing sediments, Mackenzie Delta, Canada; Society of Exploration Geophysicists, SEG Expanded Abstracts, v. 21, p. 696–698.

De Pascale, G.P., Pollard, W.H., and Williams, K.K., 2008. Geophysical mapping of ground ice using a combination of capacitive coupled resistivity and ground-penetrating radar, Northwest Territories, Canada; Journal of Geophysical Research, v. 113, cit. no. F02S90. doi:10.1029/2006JF000585

Edwards, L.S., 1977. A modified pseudosection for resistivity and IP; Geophysics, v. 42, p. 1020–1036. doi:10.1190/1.1440762

Farquharson, C.G. and Oldenburg, D.W., 1998. Non-linear inversion using general measures of data misfit and model structure; Geophysical Journal International, v. 134, p. 213–227. doi:10.1046/j.1365-246x.1998.00555.x

Fortier, R. and Savard, C., 2010. Engineering geophysical investigation of permafrost conditions underneath airfield embankments in Northern Quebec (Canada); Proceedings of the Sixth Canadian Conference on Permafrost, Calgary, p. 1307–1316.

Groom, D., 2008. Common misconceptions about capacitively-coupled resistivity (CCR): What it is and how it works; Environmental and Engineering Geophysical Society, Symposium on the Application of Geophysics to Environmental and Engineering Problems, p. 1345–1350.

Hauck, C., 2006. Application of capacitively-coupled and DC electrical resistivity imaging for mountain permafrost studies; Permafrost and Periglacial Processes, v. 17, p. 169–177. doi:10.1002/ppp.555

Hunter, J.A., 2007. Development of a capacitive-coupled resistivity method for permafrost surveys in North America: Melinki Russkas (A little Russian tale); Fast Times, v. 12, no. 4, p. 23–26.

Kuras, O., Beamish, D., Meldrum, P.I., and Ogilvy, R.D., 2006. Fundamentals of the capacitive resistivity technique; Geophysics, v. 71, no. 3, p. G135–G152. doi:10.1190/1.2194892

LeBlanc, A.-M., Short, N., Oldenborger, G.A., Mathon-Dufour, V., and Allard, M., 2012. Geophysical investigation and InSAR mapping for permafrost and ground movement characterization at the airport of Iqaluit; 15th International Conference on Cold Regions Engineering, p. 644–654.

LeBlanc, A.-M., Mathon-Dufour, V., Allard, M., Oldenborger, G.A., Short, N., L'Hérault, E., and Sladen, W.E., 2013. Permafrost characterization at the Iqaluit International Airport, Nunavut, in support of decision-making and planning; Canada-Nunavut Geoscience Office, Summary of Activities 2012, p. 131–142.

Loke, M.H., Acworth, I., and Dahlin, T., 2003. A comparison of smooth and blocky inversion methods in 2D electrical imaging surveys; Exploration Geophysics, v. 34, p. 182–187. doi:10.1071/EG03182

McNeil, J.D., 1980. Electromagnetic terrain conductivity measurements at low induction numbers; Geonics Ltd., Technical Note TN-6.

Neukirch, M. and Klitzsch, N., 2010. Inverting capacitive resistivity (line electrode) measurements with direct current inversion programs; Vadose Zone Journal, v. 9, p. 882–892. doi:10.2136/vzj2009.0164

Oldenborger, G.A., 2010. Electrical geophysics applied to assessing permafrost conditions in Pangnirtung, Nunavut; Geological Survey of Canada, Open File 6725, 41 p. doi:10.4095/287267

Oldenborger, G.A., Routh, P.S., and Knoll, M.D., 2005. Sensitivity of electrical resistivity tomography data to electrode position errors; Geophysical Journal International, v. 163, p. 1–9. doi:10.1111/j.1365-246X.2005.02714.x

Scott, W.J., Sellmann, P.V., and Hunter, J.A., 1990. Geophysics in the study of permafrost; *in* Geotechnical and Environmental Geophysics, (ed.) S.H. Ward; Society of Exploration Geophysicists, Investigations in Geophysics, no. 5, p. 355–384.

Timofeev, V.M., Rogozinski, A.W., Hunter, J.A., and Douma, M., 1994. A new ground resistivity method for engineering and environmental geophysics; Environmental and Engineering Geophysical Society, Symposium on the Application of Geophysics to Environmental and Engineering Problems, p. 701–715.

Wilkinson, P., Chambers, J., Kuras, O., Meldrum, P., and Gunn, D., 2011. Long-term time-lapse geoelectrical monitoring; First Break, v. 29, p. 77–84.

Geological Survey of Canada Project 343202NP21